Available online at www.sciencedirect.com
ScienceDirect
Journal of Molecular Catalysis A: Chemical 264 (2007) 192–201
JOURNAL OF MOLECULAR CATALYSIS A: CHEMICAL
www.elsevier.com/locate/molcata

On the mutual interactions between noble metal crystallites and zeolitic supports and their impacts on catalysis

J.I. Villegas [a], D. Kubička [a,b], H. Karhu [c], H. Österholm [d], N. Kumar [a], T. Salmi [a], D.Yu. Murzin [a,*]

[a] *Laboratory of Industrial Chemistry, Process Chemistry Centre, Åbo Akademi University, Biskopsgatan 8, FIN-20500 Åbo/Turku, Finland*
[b] *VÚAnCh, Department of Refinery and Petrochemical Research, 43670 Litvínov, Czech Republic*
[c] *Department of Physics, Turku University, Vesilinnantie 5, FIN-20014 Åbo/Turku, Finland*
[d] *Neste Oil Oy, POB 310 Borgå, Finland*

Received 16 August 2006; received in revised form 6 September 2006; accepted 7 September 2006
Available online 16 September 2006

Abstract

The mutual metal–support interactions were studied in mordenite zeolite modified with 0.5, 2 and 5 wt.% platinum by impregnation or ion-exchange method. Each modification method led to different catalysts from the point of view of acidity. These interactions were thoroughly investigated by XPS, CO and pyridine FTIR spectroscopy, NH_3-TPD and a model reaction (isomerization of *n*-butane). By XPS measurements and CO adsorption, it was observed that the Pt binding energy and the CO adsorption band increased with the acidity of the support. Simultaneously, a rearrangement on the strength of acid sites was recorded by pyridine-FTIR when the zeolites were modified by a metal function. Ultimately, such changes in acidity were translated into different catalytic performances, mostly by suppressing or favoring cracking reactions. The interatomic model was examined and extrapolated to cover the effects that the metal particles have upon the support acidity.
© 2006 Elsevier B.V. All rights reserved.

Keywords: Interatomic potential model; Zeolites; Mutual metal–support interactions

1. Introduction

Supported noble metal catalysts are used in a large number of commercial applications, ranging all the way from hydrogenation/dehydrogenation, naphtha refining, hydrocracking, ring opening and isomerization to automotive exhaust after-treatment [1–7]. The metal function besides opening new reaction pathways, *e.g.* (de)hydrogenation path for isomerization, is also able to improve the catalytic stability by inhibiting the formation of carbonaceous deposits (coke) inside the pores [1–4]. The key factor in designing metal-supported zeolitic catalysts lies not only on the deep understanding of the reaction mechanism and the role of the noble metal particles in certain steps of the reaction [8] but also on the metal (zeolitic)–support synergetic interaction. Even though, it is well known that zeolitic catalysts become bifunctional, *i.e.* capable of catalyzing different types of reactions on two different active sites, once they have been modified by a metal function, a model that completely fulfills the observed effects of the zeolitic support on the metal particles and *vice versa* is still a matter of ongoing discussion [9–21]. These observed effects are mostly related to steric constrains on the morphology of zeolites, influencing their catalytic property. Nonetheless, a change on the electronic properties of the zeolite-supported metals is visible and it is a far more interesting and controversial issue ever since Dalla Betta and Boudart [22] first reported the electron deficiency of a Pt cluster supported on an acidic support. Nowadays, a wide range of sophisticated physicochemical techniques is available for a thorough characterization of supported metals, especially small metal clusters. Within these characterization techniques, IR spectroscopy still remains as one of the most informative and simple techniques that has shed more light onto the understanding of these inter-

* Corresponding author. Fax: +358 2 215 4479.
E-mail address: dmurzin@abo.fi (D.Yu. Murzin).

1381-1169/$ – see front matter © 2006 Elsevier B.V. All rights reserved.
doi:10.1016/j.molcata.2006.09.017

actions [8]. Furthermore, quantum chemical calculations seem to be gaining more momentum as complementary, but powerful, tools for the comprehension of these phenomena even though there are only few reports on zeolite-supported metal clusters [10,23–25].

In general, most of the explanations given to the mutual interaction between the support and metal particles have been deduced based on small shifts of the CO stretching frequency during CO adsorption studies on supported metals. It has been suggested that metal clusters are electron-deficient and that are indeed responsible for interesting catalytic properties observed. Such electron deficiency has been explained either by a delocalization of the support proton on the metal particles, forming a metal–proton adduct [22,26–28] or by an electron transfer between (zeolitic) support oxygen atom and the nearby metal particles [29]. It is worth noting that the former model is not able to account for the increase in electron density on metal clusters supported on alkaline zeolites, where acidic hydroxyls are not present. According to HFS-LCAO calculations, there is no net change in the electron density of the metal cluster; however, the polarization of electron density near neighboring cations leaves the metal atoms at the opposite surface electron-deficient [25]. Using state-of-the-art spectroscopic techniques such as XPS, atomic XAFS and Pt–H shape resonance, a new (interatomic) model was put forward based mainly on electrostatic Coulomb attractions between metal particles and support oxygen ions, shifting the energy of the metal valence orbitals [14–19]. Recently, several publications have validated this model for zeolitic supports with different acidities and structures [9,10,12]. Despite these different interpretations, all supporting data are in very good agreement with each other.

In this work, the nature of the metal–support mutual interaction on Pt–impregnated (or ion-exchanged) mordenite catalysts that affects both the electronic properties of the supported metals and zeolite acidity, and in turn changes the catalytic activity, has been investigated by means of XPS, CO and pyridine FTIR spectroscopy, NH_3-TPD and a model reaction (isomerization of *n*-butane). The interatomic potential model will be used to describe the observed effects.

2. Experimental

2.1. Catalyst synthesis and modification

NH_4^+-MOR-20 (CBV21A) catalyst was supplied by Zeolyst International. Two post-synthetic modifications were followed, *i.e.* impregnation and ion-exchange, in order to obtain a loading of platinum on the catalysts equal to 0.5, 2 and 5 wt.%. The impregnation procedure was accomplished by transforming the ammonium-form zeolites into their corresponding proton forms through a step calcination procedure at 773 K in a muffle oven. The prepared proton-form catalysts were impregnated with an aqueous solution of hexachloroplatinic acid (H_2PtCl_6) in a rotavapor. The post-synthetic modification was accomplished after drying the impregnated zeolites at 383 K. On the other hand, ion-exchange modifications proceeded using an aqueous solution of tetraamineplatinum(II) nitrate ($[Pt(NH_3)_4](NO_3)_2$). Typically, 4 g of the (ammonium-form) zeolite powder was suspended in 1 L of deionized water containing the metal precursor. The solution was stirred vigorously at room temperature (RT) for 24 h. Subsequently, the support was filtered and thoroughly washed with deionized water in order to remove nitrates, exchanged cations and non-exchanged precursor. Filtering and washing was repeated several times. Finally, the ion-exchanged zeolite was dried in an oven at 373 K for 24 h. It was confirmed by X-ray diffraction (XRD) that the zeolitic structures were intact after the metal modification. The Pt loading of the catalysts was determined by direct current plasma (DCP) method.

2.2. Treatments after post-synthetic metal modification

Ion-exchanged catalysts were calcined prior to any testing. The calcination procedure was performed in a fixed-bed reactor at 623 K under high flow of synthetic air (1 L/min g) with a heating rate of 0.2 K/min. High flow conditions enhance the desorption rate of water and ammonia. Such calcination conditions have been reported to markedly improve the metal dispersion [30]. After calcination, all samples were quenched to RT and reduced in hydrogen at 623 K for 1 h with a heating rate of 5 K/min. Impregnated samples were directly reduced, without any prior calcination, at the same conditions.

The resulting materials were then referred to as Pt–MOR-IMP, for impregnated mordenites, and Pt–MOR-IE, for ion-exchanged ones. When referring to a specific metal loading, a prefix with the (nominal) loading would be added to the tag name, *e.g.* 0.5 wt.% Pt–MOR-IE.

2.3. Catalyst characterization

The catalysts were characterized by direct current plasma (DCP), nitrogen adsorption, X-ray photoelectron spectroscopy (XPS), Fourier-transform infrared spectroscopy (FTIR) and CO chemisorption.

The specific surface area of the fresh Pt-modified mordenite catalysts was measured by nitrogen adsorption method (Sorptometer 1900, Carlo Erba instruments). The catalysts were outgassed at 473 K prior to the measurements and the Dubinin equation was used to calculate the specific surface area.

A Perkin-Elmer PHI 5400 ESCA equipment was used for the X-ray photoelectron spectroscopy (XPS) analysis for Pt-modified zeolitic catalysts. The catalysts were reduced *ex situ* under hydrogen at 623 K for 2 h, with a heating/cooling rate of 5 K/min. A pass energy of 44.75 eV and a measurement time of 180 min were used in order to obtain spectra with a good signal-to-noise ratio. Pressure in the vacuum chamber was 7×10^{-9} mbar during the analysis. A flood gun was used to prevent the sample from charging under X-ray bombardment. Using a glove box containing N_2 or Ar gas, a thin layer of catalyst powder was carefully smeared over a two-sided carbon tape to minimize the charging, but the possibility of minor differential charging cannot be completely ruled out. The samples were transferred to the XPS system under N_2 or Ar atmosphere. The precision of binding energies from the line fitting process is ca. ±0.1 eV. Carbon 1s peak at 284.6 eV was initially used

as binding energy reference and average values of 102.7 and 531.7 eV were obtained for Si 2p and O 1s from all of the catalysts. Since Si 2p and O 1s values were found not to correlate to differences in catalyst preparation, they were used as additional information in positioning the BE axis. The BE axis was adjusted in a way that the sum of C 1s, O 1s and Si 2p binding energies was 919.0 ± 0.1 eV. The angle between the X-ray light and the analyzer was 90° and sensitivity factors in determining surface atomic concentration ratios were 0.193, 0.711, 4.674 and 0.283 for Al 2p, O 1s, Pt 4f and Si 2p, respectively [31]. A linear background was removed from the spectra and a mixture of Gaussian and Lorentzian peak shapes was used in the line fitting procedure. Platinum $4f_{7/2}/4f_{5/2}$ intensity ratio was set to 4:3 and the BE difference was 3.33 eV. Accuracy of the atomic concentrations is considered to be ca. 20%, since the photoionization cross-sections may depend on the chemical state. Note that a prolonged XPS scan was made for chlorine or ammonium residues from the precursor solutions but none were found.

The adsorption of CO on all the platinum-modified zeolitic catalysts was investigated by infrared spectroscopy (ATI Mattson FTIR). The catalyst samples were pressed into self-supported wafers and reduced *in situ* in an FTIR cell in flowing hydrogen (AGA, 99.999%) at 623 K for 1 h. After the reduction, the FTIR cell was evacuated for 30 min at the reduction temperature. The reduced samples were then cooled to RT (298 K). The spectral background was measured, after which the samples were in contact with a flow of 10% CO in He for 30 min. Following a short evacuation (ca. 10 min) at RT, the spectra of adsorbed CO on the Pt particles, which are supported on the studied catalysts, were collected. The shift in the position of the linearly bound CO (2070–2090 cm^{-1}) was used to evaluate the interaction between Pt and the support. All spectra were recorded with a resolution of 2 cm^{-1}. The ratio of the linearly bound CO to the bridge-bound CO (1700–1900 cm^{-1}) indicated that the adsorption of CO on Pt and the areas of the peaks, which correspond to the amount of surface Pt atoms, were compared with the results obtained by dispersion measurements.

The acidity of investigated samples was measured by infrared spectroscopy (ATI Mattson FTIR) by using pyridine (≥99.5%, a.r.) as a probe molecule for qualitative and quantitative determination of both Brønsted and Lewis acid sites. The samples were pressed into self-supported pellets (12–17 mg/cm^2), set into the FTIR cell and reduced at 623 K for 1 h. The sample was then cooled down to 373 K, evacuated for 30 min and background spectra were measured before Py adsorption. Pyridine was first adsorbed for 30 min at 373 K and then desorbed *in vacuo* at different temperatures (523, 623 and 723 K) to obtain a distribution of acid sites strengths. All spectra were recorded at 373 K with a spectral resolution of 2 cm^{-1}. Spectral bands at 1545 and 1450 cm^{-1} were respectively used to identify Brønsted (BAS) and Lewis acid sites (LAS). The amount of BAS and LAS were calculated from the intensities of corresponding spectral bands by using the molar extinction coefficients reported by Emeis [32]. The low transmittance in the range of the OH vibration hinders the direct observation of Brønsted acidity by FTIR.

Additionally, the total acidities of the ion-exchanged materials were determined using temperature-programmed desorption of ammonia (NH_3-TPD) in an AMI-100 instrument (Altamira Instruments Zeton Inc.) equipped with a thermal conductivity detector (TCD). Dried samples (ca. 30 mg) were placed in the sample tube, pretreated in helium flow (AGA, 99.9999%) at 353 K for 20 min and ramped to 773 K at a rate of 20 K/min, where it was maintained for 1 h. The sample was cooled to 473 K and ammonia (AGA, 10% NH_3 in helium) was adsorbed for 1 h. The sample was flushed with helium for 1 h at 473 K and then cooled to 373 K in helium before the NH_3 desorption began. The TPD temperature profile was as follows: dwelling at 373 K for 30 min, heating to 773 K at a rate of 20 K/min, maintaining such temperature for 30 min.

Metal dispersion measurements were performed with Micromeritics TPD/TPR AutoChem 2910 equipment and quantified from the amount of chemisorbed CO (AGA, 99.997%) using a pulse method. The sample (100–150 mg) was heated with a rate of 10 K/min until 393 K and the temperature was hold for 30 min under helium atmosphere (AGA, 99.9999%). Then, the catalyst was reduced by hydrogen (AGA, 99.9999%, 20 mL/min), while the temperature was increased to 623 K in two steps: firstly to 493 K and then to 623 K with a rate of 10 K/min, the temperatures were hold for 30 min and 120 min, respectively. After the reduction, the sample was maintained under He for 90 min at 623 K. The temperature was quickly decreased to room temperature. Immediately, CO adsorption began using pulses of 0.07 mL (10% of CO in He) every 5 min while keeping the temperature constant at 303 K with the help of a water bath. The outlet gas, which passed through the sample, was led into a TC detector and the concentration of CO was recorded until the value was constant. The calculation of the dispersion based on the cumulated amount of carbon monoxide assumed the stoichiometry of CO to platinum to be the unity as confirmed by FTIR measurements.

2.4. Catalytic testing

The performance of the catalysts in the transformation of *n*-butane to isobutane was tested in a fixed-bed minireactor at atmospheric pressure with reaction temperature and weight-hourly space-velocity (WHSV) equal to 623 K and 3.5 h^{-1}, respectively. Both impregnated and ion-exchanged mordenite catalysts were pressed into pellets, crushed and sieved. A sieve fraction of 150–250 μm was collected to prevent internal diffusion in catalytic testing and dispersion measurements. The catalyst was then packed in the reactor and the reactant was fed into the reactor with hydrogen, obtaining a partial pressure of the reactant equal to 0.2 atm. Product analysis was carried out using a gas chromatograph (Varian 3700) equipped with a 50 m × 32 mm capillary column and a FI-detector (i.d. fused silica PLOT Al_2O_3–KCl). The catalyst samples were heated to 623 K with a rate of 1 K/min under H_2 flow and maintain for 1 h in order to desorb water and reduce the sample. Conversion measurements performed with different flows and amounts of catalysts at constant residence times confirmed that no external diffusion limitations took place.

3. Results and discussion

3.1. Effect of the support and metal-modification method on the electronic properties of supported Pt

Alteration of the electronic properties of supported metals by the support is a phenomenon that has been widely reported in the literature for a variety of supports, among them metal oxides, such as TiO_2, and zeolites [33,34]. However, reducible metal oxides fall outside the scope of this work given that only the metal–support interactions in zeolite-supported metals will be addressed.

In the present study, XPS and FTIR spectroscopy of adsorbed CO were used to investigate the interactions between platinum crystallites and its zeolitic support as well as to describe the influence of the metal-modification method on the supported platinum clusters. Depending on the binding energy of the supported metal, obtained by XPS, the band position of adsorbed CO shifts to higher wavenumbers as the nature of the support becomes more acidic [14]. Two regions of adsorbed CO can be assigned, at higher wavenumbers, an adsorption band due to linearly coordinated CO and at lower ones, adsorption due to CO in bridge coordination. Moreover, the integrated intensity ratio of linear to bridged-bonded CO (L/B ratio) decreases as the alkalinity of the supported increases, which means that bridged bonded CO increases at the expense of linear CO when the supported metal exhibit lower binding energy, *i.e.* less acidic.

Table 1 contains general information about the catalysts tested. Throughout this work, the nominal loading of Pt will be referred to given that DCP measurements confirmed that the actual content of Pt on the catalyst deviated from the nominal value in less than 5% for any of the metal-loading procedures.

The specific surface area of the Pt-modified zeolites, whether impregnated or ion-exchanged, remained relatively high (>530 m^2/g) even if a decrease in comparison to the proton-form is noticed (Table 1) due probably to blockage of some micropores. It can be expected that the decrease on the specific surface area will not affect the catalytic activity of the Pt–mordenite as it has been reported elsewhere [1,2].

The Pt $4f_{7/2}$ XPS spectra from the impregnated and ion-exchanged Pt–mordenite are shown in Fig. 1 while numeric values of the binding energy (BE) of Pt $4f_{7/2}$ are reported in Table 2. Clearly, the BE of Pt $4f_{7/2}$ shifts to higher values for all the materials in comparison to that of single platinum crystallites (Pt^0, ca. 71.1 eV) reported by Moulder et al. [31]. Ion-exchanged Pt-catalysts exhibited a higher binding energy, indicating a more oxidized state of the noble metal particle, which ultimately may depend on the method chosen for metal modification (Table 2). On the other hand, their Pt/Si surface atomic concentration ratios were lower. Moreover, these materials prepared by ion-exchange had higher BE than those in catalysts prepared by impregnation, which is attributed to the relatively smaller size of active metal particles. The shift of the BE is more pronounced on all Pt–MOR-IE, which possessed higher acidity than their impregnated counterparts (Table 3). However, nothing conclusive can be said in relation to the acidity and the BE of Pt $4f_{7/2}$ when trying to analyze impregnated (or ion-exchanged) Pt–MOR with different metal loadings given that the BE depends on the metal particle size, which increases with the Pt-loading (Table 2). In that sense, the highest BE of Pt was obtained on 0.5 wt.% Pt–MOR-IE and it is partly attributed to its Pt particle sizes that were the smallest ones, confirmed by CO chemisorption. By narrowing the range of the metal particle size (ca. 2 nm), the effect of the metal particle size is minimized and thus the comparison of 0.5 and 2 wt.% Pt–MOR-IMP along with 2 wt.% Pt–MOR-IE is feasible. Among such materials, the increase of the BE of Pt is

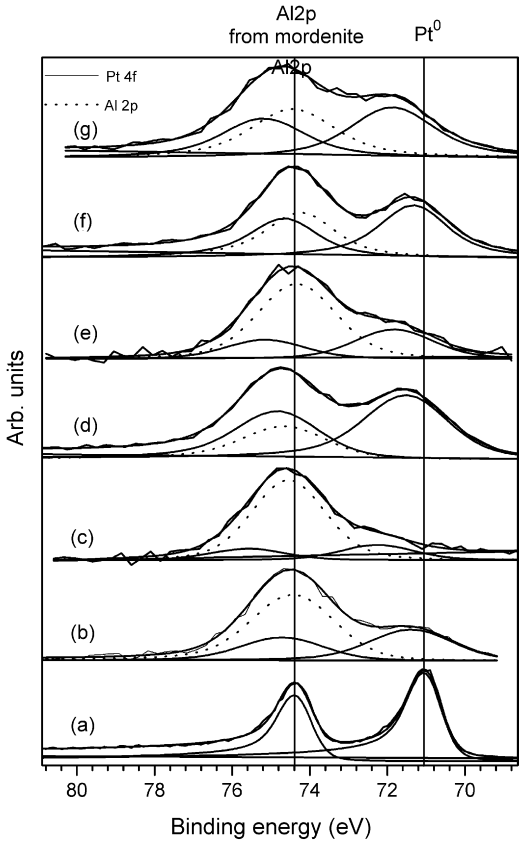

Fig. 1. Deconvolutions of Pt $4f_{7/2}$ and Al 2p lines from (a) Pt (1 1 1) single crystal, (b) 0.5 wt.% Pt–MOR-IMP, (c) 0.5 wt.% Pt–MOR-IE, (d) 2 wt.% Pt–MOR-IMP, (e) 2 wt.% Pt–MOR-IE, (f) 5 wt.% Pt–MOR-IMP and (g) 5 wt.% Pt–MOR-IE.

Table 1
General physical properties of the studied catalysts

Catalyst	SiO_2/Al_2O_3 (mol/mol)	Pt content (wt.%)	Specific surface area[a] (m^2/g)
H–MOR	20	0	605
Pt–MOR-IMP[b]	20	0.5	–
		2	569
		5	539
Pt–MOR-IE[c]	20	0.5	556
		2	–
		5	535

[a] Dubinin equation.
[b] Obtained from proton-form mordenite.
[c] Obtained from ammonium-form mordenite.

Table 2
Characterization of Pt-modified mordenite catalysts by XPS and Co adsorption

Catalyst	Pt content (wt.%)	XPS			CO pulse chemisorption[c]			CO on Pt by FTIR spectroscopy	
		Pt binding energy[a,b] (eV)	Atomic Pt/Si ratio	Atomic Si/Al ratio	Pt dispersion (%)	Relative dispersion	Average crystallite size (nm)	Position of peak maximum[d] (cm^{-1})	Relative peak area
Pt–MOR-IMP	0.5	71.4	0.0039	16.7	57.0	1.04	2.0	2079	1.12
	2	71.5	0.014	9.9	53.8	0.98	2.1	2080	0.99
	5	71.3	0.010	8.1	38.9	–	2.9	–	–
Pt–MOR-IE	0.5	72.2	0.00088	14	100	1.82	1.0	2085	2.50
	2	71.8	0.0024	12.9	55.0	1	2.0	2081	1
	5	71.9	0.0059	13.7	40.9	–	2.8	–	–

[a] Pt $4f_{7/2}$.
[b] Accuracy = 0.1 eV.
[c] Assuming spherical particles and CO/Pt stoichiometry equal to unity.
[d] Accuracy = 2 cm^{-1}.

undoubtedly due to the increase of acidity of the support and it evidences the interaction between platinum crystallites and the (zeolitic) support [8,9,14,19]. Silicon/aluminum surface atomic concentrations ratios were higher in ion-exchanged Pt–MOR catalysts (Table 2). This is either due to the difference in the photoionization cross-sections, owing to calcination conditions, or due to surface enrichment during the formation of the zeolite. However, a change in the photoionization cross-section might have taken place as a result of a change in the oxidation state of aluminum atoms in ion-exchanged Pt–mordenites when compared to Pt–impregnated mordenites.

Shifts in the CO stretching frequency obtained by IR spectroscopy are usually taken in the literature as proof of changes in the electronic properties of the (zeolite) supported metals [9,14,19]. Similarly to XPS measurements, interpretation of the results may be somehow complicated since the exact frequency of CO adsorption bands depends on the particle size, surface coverage and electronic changes in the metal structure [8,14,19]. The position of the CO adsorption peak maximum as obtained by FTIR spectroscopy is summarized in Table 2 for samples with similar metal particle size (2–2.1 nm) and rather different acidity (253–528 μmol/g). It is observed that the CO adsorption band slightly shifts to higher wavenumbers as the acidity of the catalyst increases. Koningsberger and co-workers [19] reported higher shifts for a wider range of support acidities. In order to exemplify the impact of the particle size, 0.5 wt.% Pt–MOR-IE (1 nm) that was not as acidic as 2 wt.% Pt–MOR-IE (2 nm) presented the biggest CO stretching. XPS and CO adsorption results were in good correlation with each other. Furthermore, CO spectra obtained for all the Pt-modified materials revealed that most of the CO was almost exclusively adsorbed linearly given that that bridged-bonded CO was very scarce. Therefore, the assumption that the CO/metal stoichiometry was equal to unity is completely legitimate. In addition, investigation of CO adsorption on Pt by FTIR spectroscopy can be utilized to determine the dispersion of supported Pt. The relative area of the linearly bonded CO can be then compared to the relative dispersion obtained by CO chemisorption. In that sense, Table 2 demonstrates that, once the metal particle is approximately the same (2 nm), the relative dispersion and the relative peak area obtained by these two techniques is in very good agreement.

After thoroughly analyzing and minimizing any disturbance, *e.g.* metal particle size, it can be concluded that the electronic properties of the metal crystallites are affected by the support and clearly depends on its acidity.

3.2. Influence of the zeolite-supported metal particles on the acidic properties of the support

As discussed before, the alterations of the electronic properties of metal crystallites by the support have been mainly documented, neglecting somehow the opposite case, where important properties of the particular (zeolitic) support, *e.g.* acidity, are altered by the supported metals. Evidence of such effect of sup-

Table 3
Brønsted and Lewis acidities of fresh catalysts

Catalyst	Pt content (wt.%)	Brønsted acid sites (μmol/g)			Lewis acid sites (μmol/g)		
		523 K	623 K	723 K	523 K	623 K	723 K
H–MOR	0	339	299	228	30	35	37
Pt–MOR-IMP	0.5	253	217	0	52	0	0
	2	290	50	0	44	0	0
	5	361	341	0	27	0	0
Pt–MOR-IE	0.5	413	332	0	25	0	0
	2	528	314	0	32	0	0
	5	586	239	0	29	0	0

ported metals on the acidic properties has been recognized to a very small extent [9,35–38]. One of the main objectives of this work was not only to demonstrate that the acidic properties of a zeolitic support can be modified by supporting metal particles either by impregnation or ion-exchange, but also to give a plausible explanation based on the interatomic potential model. Obviously, any change on the acidity of the support due to the interaction with the metal function, besides the reactions that the metal *per se* may catalyze, could potentially lead to different catalytic performances, *i.e.* catalytic activity and selectivity, given that the metal-modification technique and after-treatment influence the final characteristics of the metal particle. In order to study the change acidic properties of the proton and Pt-modified mordenite (-IMP and -IE), pyridine was adsorbed on the catalysts and then desorbed at different temperatures to categorize the acid sites (AS) by their strength. For such purpose, FTIR was chosen as the technique to track the pyridine adsorption/desorption on the studied catalysts since it is able to characterize Brønsted and Lewis acid sites by their respective spectral bands, *i.e.* 1545 and 1450 cm^{-1}, and furthermore to quantify them.

Independently of the method employed for supporting platinum particles on mordenite, the acidity of the support had underwent dramatic changes as seen in Table 3. At first sight, the most striking alteration is the complete disappearance of strong Brønsted and Lewis acid sites (BAS), *i.e.* those that retain Py at 723 K, in comparison to the proton-form zeolite. Interestingly, the total amount of Brønsted acid sites (BAS) of Pt–mordenite, *i.e.* those that desorb Py at 523 K, generally seems to increase and such increase is more drastic on the ion-exchanged Pt–MOR. Exceptions to this observation were 0.5 and 2 wt.% Pt–MOR-IMP, which exhibited relatively lower values. The decrease of total acidity on these samples could be attributed to a partial pore blockage by Pt particles, which inhibit the access of pyridine molecules to the AS. This affirmation agrees with the specific surface area measurements (Table 1). To account for the increase of Brønsted acidity is not straightforward for impregnated mordenite catalysts; however, a plausible explanation is that new acid sites are formed through ion-exchange of non-acidic cations compensating the framework charge for protons. On the other hand for ion-exchanged materials, the gradual release of ammonia and the formation of Brønsted acidity have been well documented [21,38,39] and can be represented as

$$Pt(NH_3)_4{}^{2+} + 3O_2 \rightarrow \ PtO \ + \ 2H^+ + 2N_2 + 5H_2O$$

(upon calcination under oxygen flow)

Moreover, Pt^{+2} can react with hydrogen upon reaction

$$Pt^{2+} + H_2 \rightarrow \ Pt^0 + 2H^+$$

Together, these are the reasons of the striking increase of Brønsted acidity on ion-exchanged Pt–MOR. Note that the total acidity of the Pt–MOR catalysts rises as it depends on the amount Pt supported. In order to confirm these observations, ion-exchanged Pt–MOR were subjected to temperature-programmed desorption of ammonia (NH_3-TPD) and the NH_3-TPD profiles are exhibited in Fig. 2. Since no broadening of the desorption peak was visible in comparison to a reference TPD profile for H–mordenite [40], which is accounted for a higher heterogeneity of adsorption centers, and furthermore only one desorption peak maximum was observed for all 3 samples, *i.e.* 0.5, 2 and 5 wt.% Pt–MOR-IE, it could be concluded that the acidic strength of these catalysts is relatively the same. As reported by Murzin and co-workers for H-MCM-41 and Pt-MCM-41 [9], it is expected that H–mordenite will find instead two desorption maxima corroborating the stronger acidic character of the proton-form zeolite. A NH_3-TPD profile for H–mordenite can be found in Ref. [40]. At the same time, the desorption peak intensity increased as more platinum is supported on the zeolite catalyst, which is an evidence of a higher number of acid sites with the same relative strength.

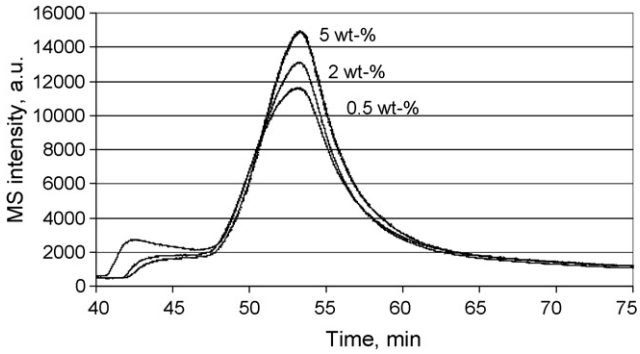

Fig. 2. NH_3-TPD profile of ion-exchanged Pt–mordenites.

Similar conclusions can be drawn for Lewis acidity. Strong and medium-strength Lewis acid sites (LAS) have completely disappeared while maintaining or increasing the total number of Lewis acid sites, *i.e.* those that retain Py at 523 K. Such slight increase can be attributed to the interaction between Pt particles and pyridine since metal crystallites are known to be acceptors of electron pairs, *i.e.* to act as Lewis acid sites. The increase of the total acidity of the Pt–MOR and disappearance of strong AS for all the Pt–MOR samples imply that Pt crystallites are able to modify the acidic strength of the zeolite. It is believed that the electronic interactions of Pt and the zeolitic support change the electron density in the conjugated base of the acid and therefore, mordenite catalysts containing reduced Pt atoms and small Pt particles are weaker from the point of view of acidity than the pure acidic counterpart, *i.e.* H–MOR.

However, in the literature alternative explanations to this phenomenon could be found [41,42]. For example, Cañizares and Carrero while studying Pt-impregnated zeolite ascribed the change on the acidity to the dealumination of the framework or to the removal of extraframework alumina by the acidic leaching [41]. It is worth clarifying that in this particular case, the plausible dealumination would be a consequence of the impregnation method with hexachloroplatinic acid. More recently, it was found for Beta zeolite that the extraction rate of extraframework alumina was much faster than framework Al under acid leaching with 1 M solution of HCl, which was translated into a decrease of LAS (followed by Py-FTIR) [42]. Since such decrease of Lewis acidity was not observed but actually the contrary was seen, such changes in acidity can be attributed solely

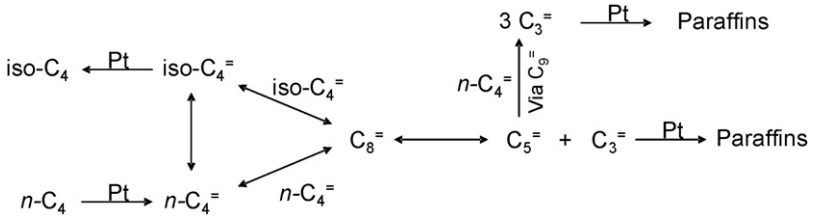

Fig. 3. Simplified scheme.

to the electronic interactions of the metal particles with the mordenite support and not to changes in the structure of the zeolite. Evidently, the ion-exchange method conditions are milder and cannot dealuminate the zeolite structure or remove extraframework Al. Thus, previous conclusions also apply to Pt–MOR-IE.

Finding out that Pt crystallites are able to modify the acidic strength of the mordenite support and keeping in mind that the average particle size ranged between 1.0 and 2.9 nm (Table 2), suggests that, at least to some extent, metal particles are located inside the zeolitic channels and close to the acid sites, given that acid sites are predominately inside the pores. Moreover, it is the only possibility to explain the observed evidences of the mutual metal–support interactions since big metal particles on the outer surface should not alter the support acidity. It is worth pointing out that the average particle size of Pt particles as obtained by CO chemisorption is calculated assuming spherical particles, thus another crystallite shapes may exist inside the pores. "Raft-like" or flat crystallites are believed to be the most predominant, which are expected to have a stronger influence on the support [8] and *vice versa*. Additionally, these "raft-like" particles must consist of only few Pt atoms given that the blockage of zeolitic pores, inhibiting the access of pyridine molecules to the acid sites, was negligible.

Several other zeolite-supported metals, such as Ir, Ru, Pd and Rh, have been recently examined and comparable tendencies were observed, where the most dramatic one was the redistribution of acidity strength, influencing the catalytic outcome of the model reactions [3,4,8,43].

3.3. Model reaction: isomerization of n-butane to isobutane

Zeolite-supported metal functions have been widely investigated for numerous hydrocarbon transformation reactions due to observed enhancements in catalytic activity and stability, which is a consequence of the reduction of carbocationic intermediates inside the pores, but also to improvements in yield and selectivity to desired products [1–4,44,45]. Nonetheless, even in the case of monofunctional reactions, *i.e.* reactions only craving the metal function, the performance of a supported metal is governed by a complex mix-up of contributions ranging from particle morphology, metal dispersion and electronic properties of the metal to redistribution of acidity strength of the support. Stakheev and Kustov have summarized some of the effects that supported metals have in different catalytic reactions, such as alkane hydrogenolysis, ring opening, hydrogenation of aromatics and isomerization of paraffins [8].

The catalytic transformation of *n*-butane to isobutane, *i.e.* isomerization of *n*-butane, over H-form and Pt-modified zeolites will ultimately confirm the alteration on the acidity strength of the (zeolitic) support. The isomerization of *n*-butane is a well known reaction [1,2] and a simplified reaction scheme can be seen in Fig. 3. Obviously, the desired product of this reaction is isobutane, which can be directly achieved by a primary carbenium ion (monomolecular mechanism) or it can be achieved through the formation of C_8 carbenium ions (bimolecular mechanism). However, the latter mechanism may also primarily account for the formation of byproducts, *i.e.* propane and pentanes. It has been widely accepted that the formed C_8 carbenium ions mainly consist of 3-methyl C_7 and 3,4-dimethyl C_6. The former carbenium ion may crack into propane and *n*-pentane as confirmed by GC analysis while the latter C_8 specie, the predominant specie, may be transformed into propane and isopentane after degradation. Moreover, the same C_8 carbenium ions are able to explain the formation of *n*-butane and isobutane after their degradation [46] (Table 4). In presence of Pt particles, the isomerization of *n*-butane can be promoted by an additional bifunctional pathway, leading to the dehydrogenation of the alkane over the metal site followed by skeletal isomerization of an olefin on acid sites and subsequent hydrogenation on metal sites. The relative importance of these mechanisms depends on the reaction temperature and the surface concentration of reactants determined by the reaction conditions and the concentration and strength of acid sites [4,47].

The dependence of the selectivity to isobutane on the conversion of *n*-butane for H–mordenite and Pt-modified mordenite can be examined in Fig. 4. The enhancement of the catalytic activity of all Pt–mordenite catalysts, either impregnated or ion-exchanged, is clear: all exhibited a higher conversion of *n*-butane

Table 4
Composition of cracking products on H–MOR and 2 wt.% Pt–MOR at TOS 10 min

Catalyst	C_1 (mass%)	C_2 (mass%)	C_3 (mass%)	isoC$_5$ (mass%)	*n*-C$_5$ (mass%)	C_3/C_5
H–MOR	0.1	12.2	39.7	2.3	1.3	3.4
Pt–MOR-IMP[a]	1.74	3.5	9.4	2.3	1.2	2.7
Pt–MOR-IE[a]	11.4	23.0	22.2	<1	<1	NA

[a] 2 wt.%.

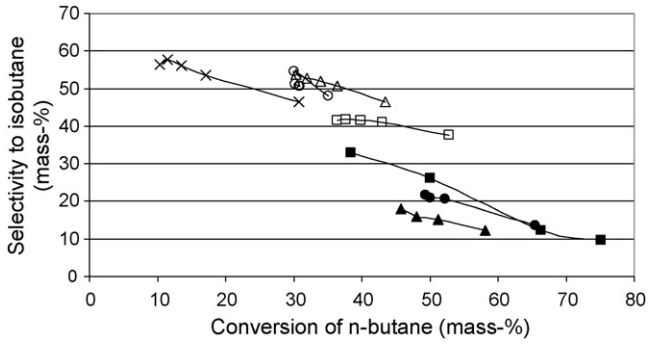

Fig. 4. Dependence of the selectivity to isobutane on the conversion of *n*-butane for H–mordenite (×) and ((△) 0.5 wt.%; (◯) 2 wt.%; (□) 5 wt.%) Pt-modified mordenite (open symbols, impregnated; filled symbols, ion-exchanged).

than H–MOR. Moreover, Pt–MOR samples seemed to be less prone to deactivate except for 5 wt.% Pt–MOR-IE, which possess the highest amount of BAS. Nevertheless, the increase of the conversion of *n*-butane did not seriously compromise the selectivity to isobutane at least over 0.5 and 2 wt.% Pt–MOR-IMP as it was for the ion-exchanged counterparts. It is worth pointing out that it is usually believed that enhancing the conversion would lead to a decrease in the selectivity to the desired product, but it is only true when the reactions are of consecutive nature. In our specific case, the selectivity to isobutane over Pt–MOR-IMP is not critically hindered since the bimolecular mechanism, which is the less selective parallel pathway, is inhibited to some extent. Moreover, these Pt–MOR-IMP samples contained relatively the same amount of acid sites as H–MOR but not the same acid strength (Table 3) since the strong acid sites were completely suppressed. As seen by FTIR measurements, all Pt-modified samples underwent a redistribution of acid site strength and did not posses strong BAS, *i.e.* those that retain Py at 723 K, thus the only plausible explanation for the inhibition of cracking reactions while increasing the catalytic activity is the change on acid strength. On the other hand, selectivity of isobutane over Pt–MOR-IE catalysts was the lowest and the conversion was the highest. Ion-exchanged Pt–mordenites not only experienced a redistribution of their acidic strength but also a dramatic increase of their respective acidity. Such increase in acidity, especially of weak BAS, might have favored the bimolecular mechanism over the monomolecular one and, consequently, cracking reactions to yield more byproducts, *i.e.* principally propane and pentane.

The composition of cracking products, *i.e.* propane and pentanes, over H- and Pt-modified mordenite may provide yet more evidence of the redistribution of acid strength that the zeolite underwent after metal modification. As mentioned before, the bimolecular mechanism involves the dimerization of two butane molecules to form C_8 carbenium ions, which could undergo isomerization and β-scisson to yield *n*- and isobutane or could disproportionate (crack) to form propane and pentanes. If no other reactions were involved in the mechanism, the ratio of produced C_3/C_5 would be close to the unity. However, such C_3/C_5 ratio is greater than unity (Table 4), behavior also observed and confirmed by kinetics studies by others [4]; the reason is that mordenite zeolite also enables C_4 and C_5 molecules to codimerize and form nonane, which readily cracks into three molecules of propane. Table 4 demonstrates that this ratio is affected by the acidity of the catalysts given that it was the highest on catalysts with the strongest acidity, *i.e.* H–MOR. In other words, the stronger the acid sites are, the higher C_3/C_5 ratio is. Alternatively, the higher C_3/C_5 ratio may be attributed to the disproportionation of butane isomers over the Pt particles under these reaction conditions and without the need of an acidic support, yielding methane and propane. However, there has been no evidence of the direct isomerization or degradation of butane molecules given that the yield to methane is relatively low for both H–MOR and Pt–MOR-IMP (Table 4). Moreover, Pt support on silica (non-acidic support) has been proven to be inactive in the isomerization of *n*-butane at the same conditions. In fact, hydrogenolysis reactions over Pt at the current conditions are feasible if and only the support is acidic enough to catalyze the reaction as observed over (2 wt.%) Pt–MOR-IE, which exhibits approximately twice as much acid sites as the impregnated counterpart.

3.4. Interactomic model for describing the metal–support mutual interactions

The following analysis is aimed at the most recent metal–support interaction model, the interatomic potential model [14], which seems to be so far the most coherent among the rest of the models that have been proposed in the literature. As mentioned before, several models have been put forward in order to describe the influence of the support on the electronic properties of Pt crystallites [22,26–29], nevertheless these models failed to incorporate the undoubtedly effect of the supported Pt particles on the properties of the (zeolitic) support, namely on the acidity, which it has been demonstrated through out this study.

The interatomic potential model is originally based on the change in the energy position of the metal valence orbitals as a result of the metal–support interaction, a decrease of the metal ionization potential with increasing the alkalinity. In this model, the main interaction is a Coulomb attraction between the metal particle and support oxygen ion, which consequently will lead to a change in the shape of the metal atomic potential caused by a variation in the electron charge of nearby support oxygen ions. Koningsberger and co-workers demonstrated that the composition of the support determined its Madelung potential, thus the electron charge of the support oxygen ions [16]. Now, if the zeolitic support is modified by a metal function, whether by impregnation, ion-exchange or another method, it is not outrageous to believe that the support Madelung potential will change. Such change will produce a cascade effect, modifying the electron charge of the support oxygen ions and eventually affecting the metal atomic potential only if the metal crystallite is located close to the acid site. By modifying the electron charge of the support oxygen, it is thus conceivable that the strength of the bond between the charge-modified oxygen ions and the non-framework proton from the bridging hydroxyl groups would also vary, which would be translated in a variation on Brønsted acidity, *i.e.* capability of donating a (non-framework) proton. Furthermore, the metal–support interface is richer in electrons

on acidic support, such as zeolites, after the introduction of a metal function and due to the richer environment of electrons at the support oxygen atoms, the hydrogen–oxygen bonds of the bridging hydroxyl groups become less ionic, *i.e.* the acidity strength decreases [9]. As evidenced, the interatomic potential model, first proposed by Koningsberger and co-workers [14], is more than capable of explaining the changes on the electronic properties of the metal crystallites and the experimentally observed alterations on the (zeolitic) support acidity.

4. Conclusions

The nature of the metal–support interactions in Pt–impregnated (or ion-exchanged) mordenite catalysts that affect both the electronic properties of the supported metals and zeolite acidity, and in turn change the catalytic activity, has been investigated by means of XPS, CO and pyridine FTIR spectroscopy, NH_3-TPD and a model reaction (isomerization of *n*-butane). It became clear that the metal–support interactions are not exclusive to the changes on the electronic properties of the supported metals. On the contrary, these are of mutual character given that the support acidity is affected by the metal modification. Also well documented in the literature, the electronic changes of the supported metals are evidenced by a shift in the CO adsorption band and an increase of the binding energy of Pt. These changes are further influenced by the acidity of the support. Simultaneously, the acidic properties of the zeolitic support change as the zeolite is modified with a metal function, *i.e.* Pt, either by impregnation or ion-exchange. Such effect is seen from the redistribution of acid sites since the strong acid sites completely disappeared while maintaining (impregnated samples) or increasing (ion-exchanged samples) the total acidity and also from their catalytic performances. Impregnation and ion-exchange preparation results in different materials with respect to their acidity, even if neither of them possessed strong acid sites, and their catalytic activity. On Pt–mordenites, the catalytic activity rose in comparison to the proton mordenite while virtually maintaining the same selectivity to isobutene (ion-exchanged Pt–MOR), which could only mean that cracking reactions are suppressed, favoring the monomolecular mechanism. Even though, Pt–MOR-IMP lacked strong acid sites, their total acidity increased abruptly favoring bimolecular mechanism (and cracking reactions) due to the higher concentration of acid sites.

Acknowledgements

This work is part of the activities at Åbo Akademi Process Chemistry Centre within the Finnish Centre of Excellence Program (2000–2001) by the Academy of Finland. Financial support from the Graduate School of Materials Research and Neste Oil for José Ignacio Villegas is gratefully acknowledged.

References

[1] J.I. Villegas, N. Kumar, T. Heikkilä, A. Smiešková, P. Hudec, T. Salmi, D.Yu. Murzin, Appl. Catal. A: Gen. 284 (2005) 223.
[2] J.I. Villegas, N. Kumar, T. Heikkilä, A. Smiešková, P. Hudec, T. Salmi, D.Yu. Murzin, Stud. Surf. Sci. Catal. 158 (2005) 1859.
[3] D. Kubička, N. Kumar, P. Mäki-Arvela, M. Tiita, V. Niemi, H. Karhu, T. Salmi, D.Yu. Murzin, J. Catal. 227 (2004) 313.
[4] V. Nieminen, M. Kangas, T. Salmi, D.Yu. Murzin, Ind. Eng. Chem. Res. 44 (2005) 471.
[5] G.D. Pirngruber, O.P.E. Zinck-Stagno, K. Seshan, J.A. Lercher, J. Catal. 190 (2000) 374.
[6] M. Guisnet, V. Fouche, M. Belloum, J.P. Bournonville, C. Travers, Appl. Catal. A: Gen. 71 (1991) 295.
[7] J. Pérez-Ramírez, J.M. García-Cortés, F. Kapteijn, G. Mul, J.A. Moulijn, C. Salinas-Martínez de Lecea, Appl. Catal. B: Environ. 29 (2001) 285.
[8] A.Yu. Stakheev, L.M. Kustov, Appl. Catal. A: Gen. 188 (1999) 3.
[9] D. Kubička, N. Kumar, T. Venäläinen, H. Karhu, I. Kubičková, H. Österholm, D.Yu. Murzin, J. Phys. Chem. B 110 (2006) 4937.
[10] P. Treesukol, K. Srisuk, J. Limtrakul, T.N. Truong, J. Phys. Chem. B 109 (2005) 11940.
[11] M.K. Oudenhuijzen, J.A. van Bokhoven, D.E. Ramaker, D.C. Koningsberger, J. Phys. Chem. B 108 (2004) 20247.
[12] Y. Ji, A.M.J. van der Eerden, V. Koot, P.J. Kooyman, J.D. Meeldijk, B.M. Weckhuysen, D.C. Koningsberger, J. Catal. 234 (2005) 376.
[13] D.C. Koningsberger, M.K. Oudenhuijzen, J. de Graaf, J.A. Bokhoven, D.E. Ramaker, J. Catal. 219 (2003) 178.
[14] B.L. Mojet, J.T. Miller, D.E. Ramaker, D.C. Koningsberger, J. Catal. 186 (1999) 373.
[15] D.C. Koningsberger, D.E. Ramaker, J.T. Miller, J. de Graaf, B.L. Mojet, Top. Catal. 15 (2001) 35.
[16] D.E. Ramaker, J. de Graaf, J.A.R. van Veen, D.C. Koningsberger, J. Catal. 203 (2001) 7.
[17] D.E. Ramaker, M. Teliska, Y. Zhang, A.Yu. Stakheev, D.C. Koningsberger, Phys. Chem. Chem. Phys. 5 (2003) 4492.
[18] D.C. Koningsberger, J. de Graaf, B.L. Mojet, D.E. Ramaker, J.T. Miller, Appl. Catal. A: Gen. 191 (2000) 205.
[19] J.T. Miller, B.L. Mojet, D.E. Ramaker, D.C. Koningsberger, Catal. Today 62 (2000) 101.
[20] M. Vaarkamp, J.T. Miller, F.S. Modica, D.C. Koningsberger, J. Catal. 163 (1996) 294.
[21] W.M.H. Sachtler, Acc. Chem. Res. 26 (1993) 383.
[22] R.A. Dalla Betta, M. Boudart, in: H. Hightower (Ed.), Proceedings of the Fifth International Congress on Catalysis, North Holland, Amsterdam, 1973, p. 1329.
[23] M.E. Grillo, M.M. Ramirez de Agudelo, J. Mol. Model 2 (1996) 183.
[24] A.L. Yakovlev, K.M. Neyman, G.M. Zhidomirov, N. Roesch, J. Phys. Chem. 100 (1996) 3482.
[25] E. Sanchez-Marco, A.P.J. Cansen, R.A. van Santen, Chem. Phys. Lett. 167 (1990) 399.
[26] S.T. Homeyer, Z. Karpiński, W.M.H. Sachtler, J. Catal. 123 (1990) 60.
[27] W.M.H. Sachtler, A.Yu. Stakheev, Catal. Today 12 (1992) 283.
[28] R.S. Weber, M. Boudart, P. Gallezot, Stud. Surf. Sci. Catal. 4 (1980) 415.
[29] A. de Mallmann, D. Barthoumeuf, J. Chem. Phys. 87 (1990) 535.
[30] J. de Graaf, A. van Dillen, K.P. de Jong, D.C. Koningsberger, J. Catal. 203 (2001) 307.
[31] J.F. Moulder, W.F. Stickle, P.E. Sobol, K.D. Bomben, Handbook of X-ray Photoelectron Spectroscopy, Perkin-Elmer Corp., Physical Electronics Division, USA, 1992.
[32] C.A. Emeis, J. Catal. 141 (1993) 347.
[33] S.J. Tauster, S.C. Fung, L. Garten, J. Am. Chem. Soc. 100 (1978) 170.
[34] K. Hayek, R. Kramer, Z. Paál, Appl. Catal. A: Gen. 162 (1997) 1.
[35] L.M. Kustov, T.V. Vasina, A.V. Ivanov, O.V. Masloboishchikova, E.V. Khelkovskaya-Sergeeva, P. Zeuthen, Stud. Surf. Sci. Catal. 101 (1996) 821.
[36] A.K. Aboul-Gheit, S.M. Abodoul-Fotouh, N.A.K. Abodoul-Gheit, Appl. Catal. A: Gen. 292 (2005) 144.
[37] A.K. Aboul-Gheit, S.M. Abodoul-Fotouh, S.M. Abdel-Hamid, N.A.K. Abodoul-Gheit, J. Mol. Catal. A: Chem. 245 (2006) 167.
[38] J. Valyon, J. Engelhardt, F. Lónyi, D. Kalló, Á. Gömöry, Appl. Catal. A: Gen. 229 (2002) 135.
[39] B. Imre, I. Hannus, Z. Kónya, I. Kiricsi, J. Mol. Struct. 651 (2003) 191.

[40] F. Lónyi, J. Valyon, Micropor. Mesopor. Mater. 47 (2001) 293.
[41] P. Cañizares, A. Carrero, Appl. Catal. A 248 (2003) 227.
[42] J.P. Marques, I. Gener, P. Ayrault, J.M. Lopes, F. Ramoa Rivero, M. Guisnet, Chem. Commun. 20 (2004) 2290.
[43] T. Løften, PhD Thesis, Norwegian University of Science and Technology, Trondheim, Norway, 2004.
[44] R.A. Asuquo, G. Eder-Mirth, K. Seshan, J.A.Z. Pieterse, J.A. Lercher, J. Catal. 168 (1997) 292.
[45] N.N. Krupina, A.L. Proskurnin, A.Z. Dorogochinskii, React. Kinet. Catal. Lett. 32 (1986) 135.
[46] R. Asuquo, G. Eder-Mirth, J.A. Lecher, J. Catal. 155 (1995) 376.
[47] T. Narbeshuber, H. Vinek, J.A. Lercher, J. Catal. 157 (1995) 388.